Single Fungal Kinesin Motor Molecules Move Processively along Microtubules

Stefan Lakämper,*†‡ Athina Kallipolitou,† Günther Woehlke,† Manfred Schliwa,† and Edgar Meyhöfer*‡
*Cellular and Molecular Physiology, Medical School Hannover, 30635 Hannover, Germany; †Adolf-Butenandt-Institute of Cell Biology, Ludwig-Maximilians-University Munich, 80336 Munich, Germany; and ‡Mechanical Engineering, University of Michigan, Ann Arbor, Michigan 48109 USA

ABSTRACT Conventional kinesins are two-headed molecular motors that move as single molecules micrometer-long distances on microtubules by using energy derived from ATP hydrolysis. The presence of two heads is a prerequisite for this processive motility, but other interacting domains, like the neck and K-loop, influence the processivity and are implicated in allowing some single-headed kinesins to move processively. *Neurospora* kinesin (NKin) is a phylogenetically distant, dimeric kinesin from *Neurospora crassa* with high gliding speed and an unusual neck domain. We quantified the processivity of NKin and compared it to human kinesin, HKin, using gliding and fluorescence-based processivity assays. Our data show that NKin is a processive motor. Single NKin molecules translocated microtubules in gliding assays on average 2.14 μm ($N = 46$). When we tracked single, fluorescently labeled NKin motors, they moved on average 1.75 μm ($N = 182$) before detaching from the microtubule, whereas HKin motors moved shorter distances (0.83 μm, $N = 229$) under identical conditions. NKin is therefore at least twice as processive as HKin. These studies, together with biochemical work, provide a basis for experiments to dissect the molecular mechanisms of processive movement.

INTRODUCTION

Kinesins are ubiquitous microtubule-based motor molecules of eukaryotic cells. They are involved in numerous cellular processes including organelle transport, chromosome segregation, and cell signaling. The founding member of the kinesin superfamily, now referred to as conventional kinesin, has been isolated from various animal tissues (Brady, 1985; Vale et al., 1985) and is structurally and functionally the best-studied member of these motor molecules. Conventional kinesins, at least of animal species, are tetrameric proteins consisting of two identical heavy and two identical light chains (Bloom et al., 1988; Scholey et al., 1989). Each heavy chain possesses a globular head at its N-terminal end that is connected via a short linker to an α-helical neck (Kozielski et al., 1997). The neck domains of the heavy chains form a two-stranded coiled-coil to dimerize both chains (de Cuevas et al., 1992; Tripet et al., 1997). Further C-terminally the heavy chains continue in a flexible hinge region followed by a stalk and a globular tail domain (Yang et al., 1989). The stalk consists of two coiled-coils that are interrupted by a second flexible hinge region. The light chains of conventional kinesin bind to the tail region (Hackney et al., 1992; Hirokawa et al., 1989) and are thought to be involved in anchoring kinesin to vesicular cargoes and in regulating the activity of the kinesin molecule (Hackney and Stock, 2000; Jiang and Sheetz, 1995; Seiler et al., 2000; Verhey and Rapoport, 2001). The light chains are not required for in vitro motility, but are necessary for in vivo function.

Conventional kinesin has received considerable attention as a model system for dissecting the molecular mechanism of motility. This interest in the kinesin system is to a large part due to the ability of single kinesin molecules to move processively micrometer-long distances along microtubules without detaching. Initial evidence for this remarkable ability came from in vitro microtubule gliding (Howard et al., 1989) and bead assays (Block et al., 1990). At low kinesin densities, microtubule gliding movement characteristically differed from that at higher densities and was suggestive of movement driven by a single motor molecule: microtubules pivoted about a single nodal point and often moved several micrometers until the trailing end of the microtubule was reached. More importantly, the observed rates of attachment and detachment of moving microtubules (landing rate) as a function of the kinesin density confirmed that the microtubule gliding at low kinesin densities was indeed due to single kinesin molecules (Howard et al., 1989). Additional support in favor of the processivity of single molecules came from laser trapping experiments showing that silica beads coated on average with less than one kinesin molecule also moved micrometer-long distances when placed on microtubules or axonemes (Block et al., 1990). Moreover, later work showed that single conventional kinesin molecules are even capable of moving processively, albeit slower, when challenged by substantial elastic force up to 5–7 pN (Hunt et al., 1994; Kojima et al., 1997; Meyhöfer and Howard, 1995; Svoboda et al., 1993; Visscher et al., 1999).

One qualm of these processivity experiments was that the motors might preferentially aggregate when adsorbing onto glass or bead surfaces. This uncertainty was dispelled by directly recording the movement of single kinesin molecules. By using low-background total internal reflection fluorescence (TIRF) microscopy Vale et al. (1996) were able to observe single, fluorescently labeled kinesin molecules while

Submitted July 8, 2002, and accepted for publication October 23, 2002.
Address reprint requests to Edgar Meyhöfer, E-mail: meyhofer@umich.edu.

0006-3495/03/03/1833/11 $2.00

translocating along microtubules, and from the bleaching behavior they could deduce that the fluorescing spots indeed represented single, labeled kinesin molecules. Taken together, the evidence for conventional kinesin being a processive motor is overwhelming.

Recently, a fungal counterpart to conventional kinesin from animal cells has been isolated from the ascomycete *Neurospora crassa* (Steinberg and Schliwa, 1995, 1996). Sequence comparison indicates that *Neurospora* kinesin (NKin) is a distant relative to conventional animal kinesins, consistent with the phylogenetic relation between fungi and animals. NKin shares the same overall molecular design plan with conventional kinesins and seems to have analogous cellular functions, despite the apparent lack of light chains. Surprisingly, however, NKin translocates microtubules in in vitro gliding assays more than three times faster than conventional animal kinesins (Steinberg and Schliwa, 1995, 1996). Because of the functional and sequence difference to conventional animal kinesins, NKin offers unique opportunities to analyze the molecular mechanisms underlying the movement of kinesins by combining, for example, domains from fungal and animal kinesins (Grummt et al., 1998a; Henningsen and Schliwa, 1997; Kallipolitou et al., 2001). As a prerequisite for such studies, it is critical to determine whether NKin is processive.

First experiments with NKin presented by Crevel et al. (1999) demonstrated a swiveling behavior of microtubules in gliding assays and runs of consecutive 8-nm steps in laser trapping experiments typical for the motile behavior of a processive kinesin. However, in contrast to in vitro assays with animal kinesins, the concentrations of NKin required for these motility assays were so high that based on the calculated surface density of motors, multiple, not single, molecule interactions are to be expected. Furthermore, observations of Inoue et al. (1997) also showed that multiple kinesins power beads in a stepwise fashion along microtubules. Therefore, despite the findings by Crevel et al. (1999), it is possible that NKin, like Ncd or Eg5, is not processive (Crevel et al., 1997; Foster and Gilbert, 2000). Alternatively, NKin might just adsorb poorly to glass surfaces or small latex beads. Therefore, we sought to determine whether NKin is indeed processive by using a method that does not depend upon the adsorption of the motor to the substrate.

Following the approach of Vale and Yanagida, we directly tracked the movements of single motors to quantitatively determine the processivity of *N. crassa* kinesin (Vale et al., 1996). We cloned a truncated *Neurospora* motor construct (NKin483), and, for comparative purposes, a human kinesin (HKin560), which consisted of the N-terminal 483 and 560 amino acid residues, respectively. Both motor molecules were engineered with a reactive cysteine residue at the C-terminus (Kallipolitou et al., 2001). Purified proteins were labeled at this residue with the fluorescent dye Cy3. To determine if these kinesin molecules are processive, we recorded the movement of single motor molecules in a low-background TIRF microscope and also analyzed their motile behavior by comparing the microtubule gliding behavior in multiple and single molecule assays. Our results not only show that NKin is capable of processive movement, but also demonstrate that NKin483 is significantly more processive than HKin560.

MATERIALS AND METHODS

Cloning and purification of proteins

Unless stated otherwise, all reagents were obtained from Sigma (St. Louis, MO, USA). All measurements were performed at saturating MgATP concentrations (1 mM MgATP or higher, $k_{0.5}^{ATP}$ for HKin and NKin is ~100–150 μM). HKin560, human kinesin truncated at residue 560, and NKin483, *N. crassa* kinesin containing the N-terminal 483 amino acid residues, with an additional peptide containing a highly reactive cysteine PSIVHRKCF (Funatsu et al., 1997; Kallipolitou et al., 2001) at their C-terminal end, were expressed in *Escherichia coli* and purified by phosphocellulose (P11, Whatman, Newton, MA, USA) and either MonoQ (Vale et al., 1996) or MonoS (Kallipolitou et al., 2001) chromatography, respectively. After determination of the protein concentration, the peptides were Cy3-labeled using a monofunctional Cy3-maleimide (Amersham Biosciences, Freiburg, Germany). Labeled functional protein was purified from the reaction solution using a microtubule-affinity protocol (Vale et al., 1985). The labeling ratio of the reactive cysteines was determined spectrophotometrically and was close to 0.8 for all preparations, resulting in an average of 1.6 fluorophores per kinesin dimer. Tubulin was purified from pig brain (modified after (Howard et al., 1993)) and nonspecifically labeled with either TMR- or Cy5-succinimidyl-esters (Molecular Probes, Eugene, OR, USA, and Amersham Bioscience, respectively). Competent, modified tubulin was extracted by repeated cycles of polymerization and depolymerization (Howard et al., 1993).

TIRF microscopy

We modified a Zeiss Axiovert 135 TV inverted microscope to observe single, fluorescently labeled kinesin motor molecules via total internal reflection fluorescence microscopy. The basic setup is shown in Fig. 1. For illumination we used the 514-nm line of an argon ion laser (Omnichrome 532 AP A01, Melles Griot, Bensheim, Germany), whose beam was coupled into a single-mode, polarization-maintaining optical fiber. On one side of the microscope stage we mounted a three-axis manipulator with a tilting stage that accepted the beam-shaping output optics of the single-mode fiber and a focusing lens. This arrangement allowed precise steering and focusing of the laser beam in the object plane, i.e., the quartz-solution interface. A second manipulator, mounted on the other side of the microscope stage, was used to position a small suprasil prism (Melles Griot) over a quartz microscope slide in the region of interest. The prism was optically coupled to a quartz slide with glycerol. The angle and position of the laser beam and position of the prism were adjusted such that the laser beam was coupled via the prism into the quartz slide at such an angle that total internal reflection took place at the quartz slide-solution interface (see Fig. 1). The laser beam was focused to a spot size of ~10 × 20 μm and the total power in the focal plane was adjusted to ~1.5 mW, resulting in an average power density of 0.01 mW/μm^2. The intensity difference of the evanescent wave over the illuminated spot was about twofold. To ensure approximately constant fluorescence excitation conditions, we always used the same central area for all assays.

Fluorescent signals were recorded with a 1.4 NA, 100× Plan-Apochromat objective (Zeiss, Göttingen, Germany). The Cy5 fluorescence from labeled microtubules was recorded with a standard filter set consisting of an FT 580 dichroic mirror and an LP 590 long-pass filter (both from Zeiss), which resulted in submaximal signal levels that were nonetheless

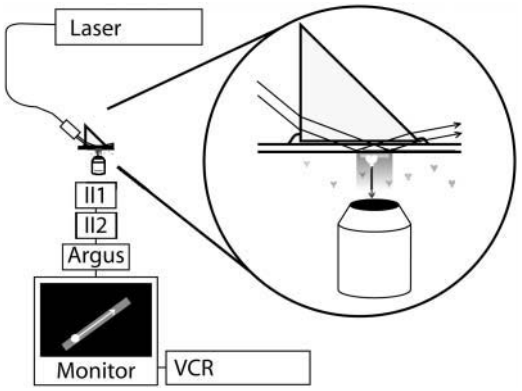

FIGURE 1 Schematic illustration of the TIRF setup. The setup was built around a modified Zeiss Axiovert 135. The beam of an argon ion laser was coupled into a single mode fiber and then projected on a suprasil prism at a low, adjustable angle. The prism was optically coupled to a quartz slide with glycerol. Total internal reflection took place at the quartz-water interface. The evanescent wave of the laser beam illuminated only a very thin layer of the assay chamber allowing us to collect fluorescence near the interface with a very low background signal. Fluorescence of both the microtubule (Cy5) and the kinesin molecules in solution (Cy3) was collected with a high numerical aperture objective (Zeiss, Plan-Apochromat, 100×, NA 1.4). After locating a microtubule, Cy5 fluorescence was blocked by a 590/75LP filter set, to collect Cy3 signal only. The signal was first amplified by a Videoscope and Hamamatsu image intensifier, and the intensified image was subsequently quantified by a CCD camera. The resulting image was filtered with an image controller (Argus) before presentation on a video monitor and storage on S-VHS-tape.

sufficient to localize microtubules. Cy3 fluorescence signals were filtered with a HQ 580/75M band pass filter (Chroma, Brattleboro, VT, USA), which blocks Cy5 fluorescence completely. In addition, scattered excitation light (514 nm, Fig. 1) was blocked with an HQ 545 LP filter (Chroma). Signals were intensified with two image intensifiers connected in series, a Videoscope VS4-1845 (Videoscope International, Dulles, VA, USA) and a Hamamatsu Image Intensifier (C2400-87, Hamamatsu Photonics, Hamamatsu, Japan). Intensified output signals were visualized with a CCD camera (C3077, Hamamatsu Photonics) and enhanced by an Argus II image processor (Hamamatsu Photonics). All raw data were stored on S-VHS videotape and analyzed afterward.

Motility assays

Motility assays at high and low motor densities were performed following standard procedures (Howard et al., 1989). Briefly, flow chambers were precoated with BRB80 (80 mM PIPES-KOH, 1 mM EGTA, 2 mM $MgCl_2$, pH 6.9) containing 0.1 mg/ml casein for 3 min, then motor dilutions in BRB80 containing 0.05 mg/ml casein were introduced and allowed to incubate for 3 min. TMR-labeled microtubules were diluted in an MgATP containing oxygen-scavenger solution (0.1 mg/ml glucose-oxidase, 0.08 mg/ml catalase, 1 mM DTT, 10 mM glucose) with additional 10 μM taxol and introduced into the flow-chamber. Microtubules were observed using an epifluorescence microscope (Axiovert 135 TV, Zeiss). For gliding assays at very low motor densities (single molecule in vitro gliding assays), microtubules were triturated to lengths of 1–5 μm by passing the solution through a 30-gauge needle before introduction into the flow chamber. Images were stored on S-VHS and analyzed afterward.

Single molecule processivity assays were performed following the procedure given in Vale et al. (1996). Briefly, fluorescently labeled motor molecules were diluted to ~5 nM in a P12 buffer (12 mM PIPES-KOH, 1 mM EGTA, 2 mM $MgCl_2$, pH 6.8) containing 30 mg/ml BSA (11930, Serva, Heidelberg, Germany). Diluted motor protein was combined with equal parts (1.1 μl each) of the following three solutions: 1), glucose-oxidase (0.4 mg/ml) and catalase (0.32 mg/ml) in P12; 2), $MgCl_2$ (4 mM), ATP (16 mM), DTT (4 mM), and glucose (40 mM) in P12; and 3), Cy5-labeled microtubules (diluted ~100-fold depending on the individual preparation) in BRB80 stabilized with 40 μM taxol, resulting in a final concentration of 29 nM PIPES. Directly after mixing, the solution was applied to a clean fused silica slide and covered with a coverglass. Processivity assays with single NKin molecules required a slight modification: instead of 4 mM ATP, the buffer contained a final concentration of 1–10 μM AMP-PNP and the solutions were incubated for ~5–15 min to allow the motor to bind to the microtubules before applying a 4-μl volume to a cleaned quartz slide. After identification of microtubules with immobilized Cy3-labeled motors, an ATP-containing solution (4 mM ATP) was washed into the chamber and the ensuing movement of the motor molecules was recorded on videotape. All motility assays, single and multiple motor microtubule gliding assays, as well as processivity assays, were carried out at 22°C ± 1°C.

Analysis of single molecule experiments

Global bleaching constants of fluorescently labeled motors were determined from frame-by-frame analysis of large assemblies of surface- or microtubule-bound motors. The change of fluorescence intensity as a function of time was analyzed using an Argus 20 image processor (Hamamatsu Photonics). The intensity of individual fluorescent spots, either surface adsorbed or moving on a microtubule, was analyzed using the same method.

The speed of motor molecules translocating along microtubules was determined by calculating the distance using a calibration standard (Leica, Wetzlar, Germany) and dividing the distance traveled by the elapsed time. All data and statistical analysis was performed using Origin 4.0 (Microcal Software, Northampton, MA, USA) or routines contained in the S-Plus programming environment (Becker et al., 1988).

RESULTS

Multiple motor gliding assays

Multiple motor in vitro gliding assays of a wild-type mammalian kinesin (porcine kinesin) and wild-type (wt)-NKin using high motor densities showed gliding speeds of 0.60 μm/s (±0.07 μm/s, $N = 24$) and 1.72 μm/s (±0.03 μm/s, $N = 48$), respectively. All errors are stated as mean ± SE. Truncated constructs of human (HKin560) and *Neurospora* (NKin483) kinesin used for the single molecule fluorescence assays transported microtubules in multiple molecule gliding assays with the same velocities as wt-motors (HKin: 0.78 ± 0.09 μm/s, $N = 101$, NKin: 1.95 ± 0.05 μm/s, $N = 20$). NKin gliding velocities were susceptible to the ionic strength of the buffer solution; microtubule gliding speeds increased from ~1.40 ± 0.07 ($N = 25$) to 2.43 ± 0.07 μm/s ($N = 25$) in P12 without salt and BRB80 with additional 400 mM KCl, respectively. Microtubule gliding assays using more than 400 mM KCl in BRB80 showed no microtubule binding to glass surfaces coated with NKin.

Single molecule gliding assays

One strategy to demonstrate processive movement of single HKin and NKin molecules was to reduce the motor density

in the gliding assays until the transport of microtubules by a single kinesin molecule could be observed (Howard et al., 1989). Reduction of the HKin560 densities on the glass surface to less than 500 molecules/μm^2 (calculation based on the assumption that all motor protein adsorbed in a functional manner) allowed observations of events where short (2–5-μm-long) microtubules bound to the surface and pivoted around a nodal point while being transported with wt-speed (0.77 μm, $\pm$ 0.03 μm/s, $N = 49$, Fig. 2 *a*). The density of Nkin483 at which single molecule gliding events could be identified was calculated to be ~5000 molecules/μm^2, much higher than for Hkin560 (Fig. 2 *b*). To address the possibility that the adsorption of NKin483 is impaired, we also attempted dilution experiments with two additional constructs that offer improved surface adsorption as compared to Nkin483: Full-length NKin, and a NKin construct in which the C-terminal portion of the motor (amino acid residues 434-483) was exchanged for the slightly longer C-terminus of HKin560 (amino acid residues 430-560). We observed single molecule gliding experiments with both constructs, but the densities that were required to effectively observe events were basically identical to those reported for NKin483.

Nonetheless, the observed motile behavior of individual NKin events was consistent with single motor events: microtubules pivoted about a single point, the rotation of the microtubule was random (diffusive) covering angular ranges up 45° in 1 s, and microtubules moved with wild-type speed relative to the nodal point (2.31 μm/s $\pm$ 0.07 μm/s, $N = 46$, BRB80 with additional 200 mM KCl, Fig. 2 *b*), suggesting that a single motor molecule is located at the nodal point. During most single motor events, microtubules abruptly dissociated from the motor before the end of the microtubule was reached (>80%). Motile events running to the end of the microtubules, which could be spatially resolved to ~0.4 μm, were excluded from the analysis. For HKin and NKin assays, no tethering of mirotubules was observed at the end of motile events, independent of whether the end of the microtubule was reached or not. Given the similar length distribution of microtubules used in single molecule gliding assays, the estimate of the average run length of NKin is more susceptible to a slight underestimation because of NKin's longer average run length. Altogether, the motile behavior shown in Fig. 2 is consistent with the hypothesis that both Hkin560 and Nkin483 are capable of processive movement. The calculated mean run lengths for Hkin and NKin from these single molecule in vitro gliding assays are 1.09 $\pm$ 0.10 μm and 2.14 $\pm$ 0.29 μm, respectively.

Single molecule fluorescence assays

To circumvent potential problems involving aggregation and adsorption, and to address the finding of unexpectedly high densities of motor molecules at which we observed single molecule microtubule gliding events, we sought to directly assay the processive movement of single, fluorescently marked motor molecules. We first quantified the bleaching behavior of our Cy3-labeled, truncated Hkin560 and Nkin483 motors in the TIRF microscope. We attached a large number of labeled motor molecules either by nonspecific adsorption or by binding microtubules decorated with labeled motor molecules to the surface of a quartz slide and recorded the TIRF signal. The fluorescence intensity was quantified over time using the Argus image processor (Fig. 3). In agreement with previous observations, the decay of the fluorescence intensity could be fitted to a single exponential function (Pierce et al., 1997; Pierce and Vale, 1998; Vale et al., 1996). From the exponential rate constants we determined the average times for bleaching fluorescently labeled NKin and HKin molecules, which were 15.9 $\pm$ 2.2 s and 18.6 $\pm$ 2.7 s, respectively (Fig. 3). In addition, we recorded the fluorescence under conditions where the fluorescently labeled motor molecules were diluted to a surface concentration below 0.1 molecules/μm^2. Under these

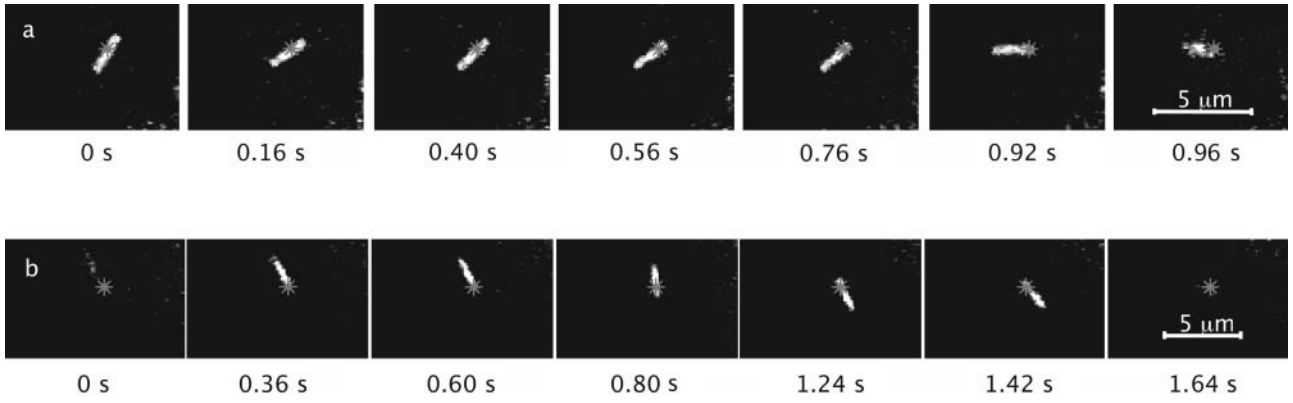

FIGURE 2 Single molecule in vitro gliding assays of HKin and NKin. The panels show typical events for the truncated constructs of HKin (*a*) and NKin (*b*). Microtubules bound to the surface and were transported unidirectionally at wt-speed (~0.8 μm/s and ~1.7 μm/s, respectively) while pivoting around a single point. Calculated densities of truncated motors on the casein pretreated glass surface were 500/μm^2 and 5000/μm^2 for HKin and NKin, respectively. For tissue-purified animal conventional kinesin (porcine kinesin), we could readily detect such events at motor densities below 5/μm^2.

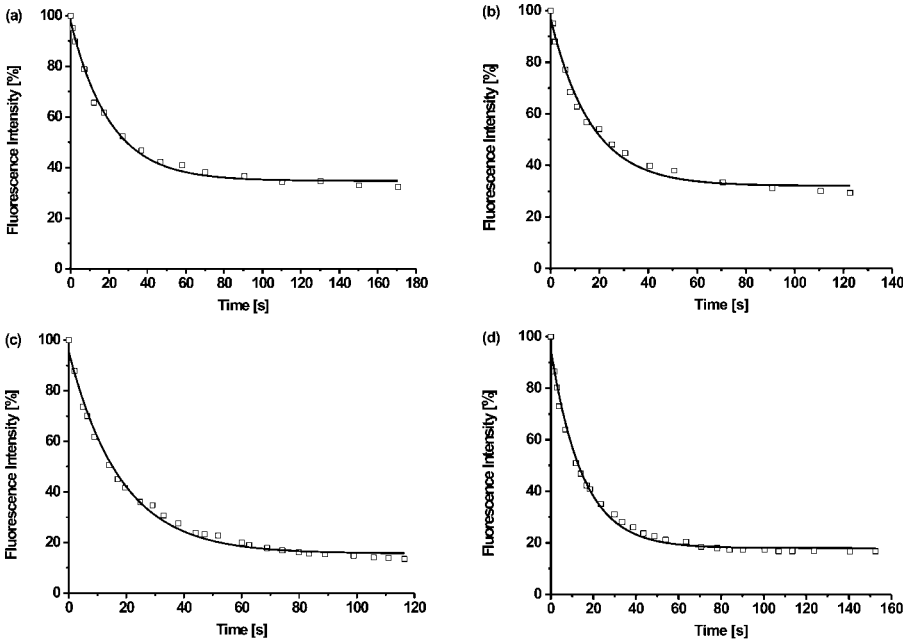

FIGURE 3 Global bleaching behavior of Cy3-marked HKin and NKin motors. The decay constants of bleaching of fluorophores covalently linked to the motor protein constructs were determined by observing several hundred fluorophores in a designated area over time, and plotting the overall intensity of the signal against time. The signal was fit to a single exponential function, yielding rate constants for bleaching. The average time for photobleaching Cy3-labeled kinesins under our conditions were 15.9 ± 2.2 s (*a* and *b*) and 18.6 ± 2.7 s (*c* and *d*) for NKin and HKin, respectively (two independent preparations each).

conditions we observed individual spots; a frame-by-frame analysis of the fluorescence intensities of these spots showed an incremental bleaching behavior, either in one or two steps, for both HKin and NKin molecules (Fig. 4 *c* and Fig. 5, *c* and *d*). A one- or two-step bleaching behavior of dimeric motor molecules is consistent with the labeling ratio of reactive cysteines of ~0.8. Roughly, we observed twice as many molecules bleaching in two steps compared to motors bleaching in one step. These observations confirm that we can resolve single molecules and that the motors do not aggregate under the conditions used in this study.

When we combined Cy5-labeled microtubules with Cy3-labeled HKin in the TIRF setup, association and movement of fluorescent spots could be observed. The spots moved with an average velocity of 0.81 ± 0.01 μm/s ($N = 229$), which is in very good agreement with the wt-speed and the velocity of the truncated HKin constructs in both multiple (0.78 ± 0.01 μm/s) and single (0.77 ± 0.03 μm/s) molecule gliding experiments. Although we also observed the same behavior for Cy3-labeled NKin483, this approach proved to be experimentally impractical as NKin associates with immobilized microtubules at such a low rate that only a small number

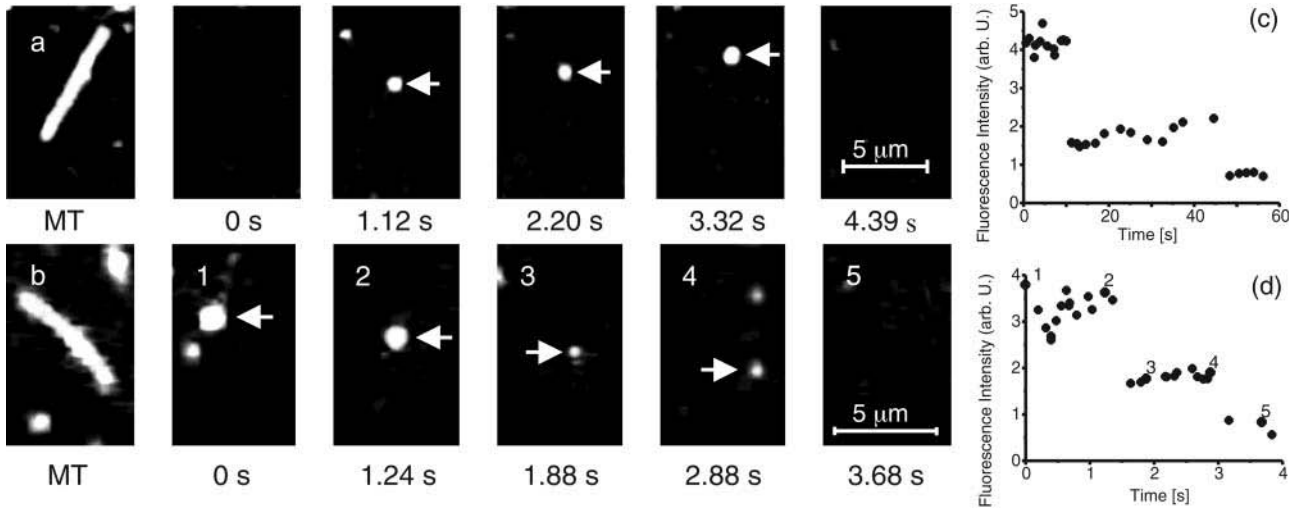

FIGURE 4 Single molecule fluorescence processivity assays for HKin. Fluorescently labeled HKin molecules were observed to bind to and move along a Cy5-marked microtubule (*a* and *b*). The gliding speed of the motor molecules (0.8 μm/s) corresponded well to the speed observed in multiple molecule gliding assays and single molecule gliding assays. Both surface adsorbed (*c*) and moving (*d*) HKin motor molecules bleached in an incremental fashion. Panel *b* shows a gliding HKin molecule bleaching in a two-step fashion. The intensity of this moving, fluorescent spot in *b* is shown in *d*. Numbered intensities in (*d*) correspond to the numbered frames in *b*.

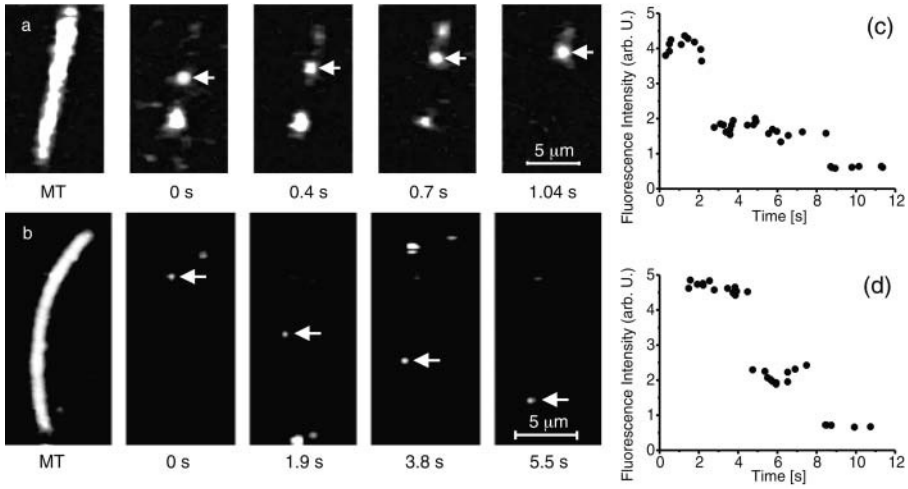

FIGURE 5 Single molecule fluorescence processivity assays for NKin. In contrast to HKin, efficient observation of single molecule movement events of fluorescently marked NKin molecules could only be observed after immobilization on microtubules by AMP-PNP and starting the assay by exchanging ATP containing buffer solution into the assay chamber. The images show smooth, unidirectional movement of a single motor at wt-speed of 1.7 μm/s (*a* and *b*). Surface-adsorbed motors were detected to bleach in incremental steps (*c* and *d*).

of processive events can be observed in this manner. However, we were able to reproducibly record processive movement of single NKin molecules on microtubules after first binding NKin to microtubules with AMP-PNP (1–10 μM) and then inducing movement by introducing an ATP-containing solution. Approximately 10% of the motors started to move. Most other fluorescent spots bleached before movement could be observed, and some spots remained stationary. Examplary events of movement are shown in Fig. 5. The velocity of moving spots was 1.70 $\pm$ 0.05 μm (N = 182), which is in good agreement with the multiple and single molecule gliding assays under low salt conditions. We also performed single molecule fluorescence assays with NKin at 200 mM KCl. The identified moving spots also moved long distances with a velocity of 2.19 $\pm$ 0.13 μm/s (N = 19), which again is in good agreement with the multiple and single molecule gliding assays in BRB80 supplemented with 200 mM KCl. To allow a direct comparison of the run lengths of HKin and NKin, we decided to measure the run lengths in buffer without additional salt.

Histograms of the run lengths of our HKin (N = 229) and NKin (N = 182) processivity assays can be fit by single exponential distributions (Fig. 6). The mean distance calculated as the decay length of the fit is 0.83 $\pm$ 0.06 μm for HKin and 1.75 $\pm$ 0.09 μm for NKin. The run length for HKin obtained here is in very good agreement with data presented by Vale et al. (1996), although they reported a much lower average velocity (0.3 μm/s) on axonemes (Thorn et al., 2000; Vale et al., 1996). To determine the number of steps a kinesin takes before dissociating from the microtubule, the travel distance was divided by 8 nm. Thus, HKin takes on average 104 steps whereas NKin takes 219 steps before dissociation from the microtubule.

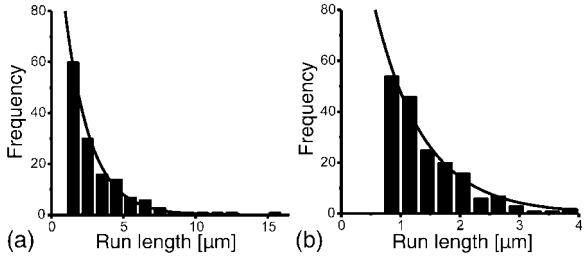

FIGURE 6 Histograms of the run lengths of HKin and NKin. Run lengths of processive movement (see Discussion) of HKin and NKin at standard buffer conditions (no additional salt) were combined in a histogram. The data were fit by a single exponential. The time constant of the exponential fit gives the mean run length of the motor molecule.

DISCUSSION

In this report we quantitatively evaluated the processive behavior of a fast fungal, microtubule-based motor molecule, *N. crassa* kinesin, NKin. We engineered a truncated, dimeric motor, NKin483, and introduced a reactive cysteine at the C-terminus for selective labeling with Cy3 dye. For comparison we also purified and labeled an analogous human kinesin construct, HKin560. Two independent methods, single molecule in vitro gliding assays and fluorescence-based single molecule assays, were exploited to quantify the processivity of both kinesins. Our observations, which are characterized by a robust quantitative agreement between the different processitivity assays, demonstrate not only that NKin is processive, but also substantiate that NKin is at least twice as processive as HKin (Table 1).

In vitro gliding assays

Initially, we attempted to quantify the processive properties of NKin by using single molecule in vitro gliding assays as first established by Howard et al. (1989). The single molecule gliding assays for NKin presented in this paper are characterized by similar motile properties: 1), the average gliding speed of NKin single motor events (~1.7 μm/s and ~2.2 μm/s with and without additional 200 mM KCl in the

TABLE 1 Comparison of the motile properties of HKin560cys and NKin483cys

	HKin560cys			NKin483cys		
Assay	Multiple molecule gliding assays	Single molecule gliding assays	Fluorescence processivity assays	Multiple molecule gliding assays	Single molecule gliding assays	Fluorescence processivity assays
Velocity	0.78 ± 0.01 μm/s ($N = 101$)	0.77 ± 0.03 μm/s ($N = 49$)	0.81 ± 0.01 μm/s ($N = 229$)	1.72 ± 0.03 μm/s ($N = 48$, wt)	n.d.	1.70 ± 0.05 μm/s ($N = 182$)
				2.20 ± 0.03 μm/s ($N = 103$) (incl. 200 mM KCl)	2.31 ± 0.07 μm/s ($N = 46$) (incl. 200 mM KCl)	2.19 ± 0.13 μm/s ($N = 19$) (incl. 200 mM KCl)
Density	High	~500/μm^2	–	High	~5000/μm^2	–
Run length	–	1.09 ± 0.01 μm	0.83 ± 0.06 μm	–	2.14 ± 0.29 μm	1.75 ± 0.09 μm

buffer solution) was unchanged compared to that in multiple molecule gliding assays, and 2), microtubules underwent substantial (ranging up to 45°) angular diffusive rotations that were consistent with the measurements of Hunt and Howard (1993) for bovine kinesin. These results suggest that NKin is also capable of processive movement along microtubules.

However, in contrast to HKin, other conventional animal kinesins or myosin V (Mehta, 2001; Mehta et al., 1999), the density of motors in the NKin assays could not be varied systematically as the frequency of single motor events dropped abruptly with reduced motor density. Therefore, we were unable to confirm via dilution experiments that single motors were driving the observed microtubule gliding. Also, our single molecule NKin gliding events were recorded at motor densities much higher than expected on the basis of previous work with animal kinesins (Crevel et al., 1999; Howard et al., 1989; Romberg and Vale, 1993). The high densities required to observe the activity of single NKin molecules, which are in complete agreement with the bead and gliding assays of Crevel et al. (1999), challenge the interpretation that this kinesin is processive (Crevel et al., 1999). On the other hand, the high NKin densities in single molecule assays could be explained if 1), the adsorption of our truncated Nkin483 construct to the glass surface is impaired, thus overestimating the number of functional kinesins, or 2), if the binding of NKin motors from solution to the microtubule is reduced dramatically. Experiments using constructs such as full-length NKin and NKin/HKin tail chimera, do not lead to significantly improved dilution behavior of NKin. Therefore we conclude, in agreement with our single molecule gliding assays (see discussion below) and a previous report (Crevel et al., 1999), that adsorption of the motor to the surface is not impaired; rather, binding of microtubules to the motor (or vice versa) near the glass surface is reduced by an unknown mechanism.

The average run length of ~1.09 μm for HKin in single molecule in vitro gliding assays agrees well with previous reports (Hancock and Howard, 1999; Howard et al., 1989; Romberg et al., 1998; Thorn et al., 2000; Tomishige and Vale, 2000; Vale et al., 1996) suggesting that the in vitro gliding approach used in this study yields reliable processivity measurements. The significantly longer average microtubule run length of NKin implies that this motor is more processive than HKin. However, this interpretation of our single molecule gliding assays is uncertain for two reasons: 1), The length of the microtubules in the NKin assays ranged from 2 to 5 μm and some of the observed events were terminated by the motor reaching the end of the microtubule rather than the microtubule dissociating from the pivoting point. We excluded these events from the analysis. 2), The actual number of molecules per μm^2 could not be reliably reduced (see above), possibly allowing more than one motor to simultaneously interact with the microtubule and thus increasing the apparent processivity. To circumvent these difficulties, we used an adsorption-independent method, the single molecule fluorescence assay first performed by Vale et al. (1996).

TIRF microscopy-based processivity assays

For our assays, truncated HKin and NKin motors were labeled at an artificially introduced, reactive cysteine residue with the fluorescent dye Cy3. As expected from the measured cysteine labeling ratio (~0.8), single- and double-labeled fluorescent spots could be detected in the TIRF microscope. The characteristic bleaching behavior and the agreement of the average lifetime of a fluorophore with the globally observed rate of fluorescence photobleaching support the conclusion that the observed fluorescent spots are indeed single kinesin motor molecules. Using our TIRF system, we were able to track the binding and subsequent movement of single, fluorescently labeled kinesins along microtubules. Kinesins moved micrometer-long distances before dissociating from the microtubule or photobleaching. First we performed single molecule fluorescence processivity assays with HKin, because HKin is the best studied model system for processive movement and therefore is best suited for a comparison with Nkin. Gliding speed and distance agreed well with both multiple and single molecule in vitro gliding assays and single molecule fluorescence processivity assays. We determined the mean run length of HKin by fitting a single exponential function to a run-length histogram calculated from all events observed for HKin. The mean run

length of 0.8 μm corresponds well to the reported values for conventional kinesin (Rice et al., 1999; Romberg et al., 1998; Thorn et al., 2000; Tomishige and Vale, 2000; Vale et al., 1996). Our single molecule fluorescence experiments with HKin and the closed agreement with the results of other groups suggest that the TIRF assay is very robust.

However, the analysis of NKin's processivity with this assay proved more difficult. Although we were able to observe single, fluorescently labeled NKin motors land, move along, and dissociate from microtubules in a manner virtually indistinguishable from HKin, these events were extremely rare. This observation agrees with our previous conclusions from gliding experiments and confirms that the initial binding of NKin to microtubules is markedly reduced as compared to HKin. To allow collection of data at a reasonable rate, we first bound labeled motors to the microtubule with 1–5 μM AMP-PNP and then started the assay by introducing an ATP-containing solution (4 mM) into the flow chamber. Approximately 10% of the fluorescently labeled motors immobilized on the microtubules started to move upon the addition of ATP. This can be accounted for by two mechanisms: 1), AMP-PNP exchanges slowly for ATP, even at high ATP concentrations. Therefore, in our experiments, many motors bleach before they start moving. 2), The kinesin-AMP-PNP state locks (at least) one head onto the microtubule. During incubation a transition of one or both heads into a rigorlike conformation is possible. Kinesin is very sensitive to such rigorlike conditions and consequently motors are bound irreversibly to microtubules. This behavior can be reduced by the addition of salt. Irreversible binding of motors is also believed to be the reason for the loss of functional protein during microtubule-binding and release protocols, where addition of salt also increases the yield substantially. The gliding speeds (1.70 μm/s and 2.19 μm/s with and without additional 200 mM KCl in the buffer solution, respectively) of fluorescently marked NKin motors in these assays were in very good agreement with speeds observed in multiple and single molecule in vitro gliding assays and demonstrate that there is no problem in exchanging AMP-PNP with saturating concentration of ATP. The increase in speed upon addition of salt is not easily explained but could, for example, be due to a weakened electrostatic interaction that is involved in a rate-limiting step in the turnover of the processive motor. These experiments also proved beyond any reasonable doubt that NKin is really a processive motor. But *how* processive is NKin compared to HKin?

We compare the processivity of HKin and NKin by generating histograms of the run length of all events and fitting the resulting density functions with a single exponential distribution. As the speed of movement for NKin is sensitive to the ionic strength of the assay buffer (Crevel et al., 1999; Steinberg and Schliwa, 1995; Steinberg and Schliwa, 1996) and we wanted to exclude any possible effect of additional salt on the processivity of NKin, we chose standard buffer conditions (P12 without additional KCl) for the direct comparison of the processivity of HKin and NKin. The mean run length of NKin determined directly from the exponential time constant was 1.75 μm. This value corresponds very well to the values obtained in single molecule in vitro gliding assays (see above; Table 1). Furthermore, observations on the biochemical processivity (k_{bi} ratio, (Hackney, 1994 and 1995; Gilbert et al., 1995 and 1998) of various NKin constructs (Kallipolitou et al., 2001) strongly support our measurements. Kallipolitou et al. (2001) showed that monomeric constructs hydrolyze few ATP molecules per diffusional encounter, whereas dimeric constructs displayed significantly larger biochemical processivity, in the range of 400. Based on the reported step size of 8 nm for NKin (Crevel et al., 1999), our measured average run length of 1.75 μm is equivalent to NKin483 taking $\sim$220 steps before dissociating from the microtubule. The difference of a factor of two between the mechanical and biochemical processivity is probably based on intrinsic differences of the bulk biochemical experiment and slight differences in the buffer conditions. As steady-state and kinetic measurements with NKin constructs are very sensitive to such changes, the data are in remarkably good agreement. Our fluorescence processivity assays not only qualitatively demonstrate that single NKin motors are processive, but also quantitatively confirm our earlier, tentative conclusion based on gliding assays that NKin is at least twice as processive as conventional animal kinesin. Is this quantitative agreement perhaps fortuitous, because the observed average run lengths of the spots will need to be corrected for the bleaching of the Cy3 fluorophores?

Other groups have corrected the apparent run length of kinesins (Rice et al., 1999; Romberg et al., 1998; Thorn et al., 2000; Tomishige and Vale, 2000; Vale et al., 1996). By showing that both the run length of the motor and the bleaching rate of the fluorescent dye are single exponential distributions, a simple correction of the observed average run length is possible. Thus the average run lengths for NKin and HKin in our experiments should be increased by 6.8% and 5.7%, respectively. The corrections are small, because in our hands the average lifetime of the fluorophores is much longer than the run time on the microtubule. When we applied such a correction to our data sets and fitted the resulting raw and corrected run length histograms with single exponential functions, it became apparent that the raw data, not the corrected data, were fit significantly better by the expected single exponential distribution. We verified this observation by using a QQ plot analysis (Venables and Ripley, 1997), which showed that the corrected histograms contained notably more events at long run length than expected. Considering that we are using dimeric kinesins with a labeling ratio of 0.8, this result is not surprising. We expect that $\sim$64% of our labeled motors contain two, and $\sim$32% contain one fluorophore. Double-labeled kinesin molecules will require bleaching of both fluorophores to be

mistaken for a dissociation event, and assuming that both fluorophores bleach independently, the probability density function for such a bleaching event is no longer a simple exponential but a jointly distributed density function (Larson, 1982). Also, this function predicts that the average lifetime of double-labeled kinesins will be 1.5 times longer than that of single-labeled motors. Given that we determined the processivity from a mixture of single- and double-labeled kinesins, all our calculations, including the most conservative estimates, indicate that the correction for the observed run length is smaller than 5% for NKin and HKin, and our best estimate for the corrected run length of NKin is 1.8 μm.

In summary, both single molecule in vitro gliding assays and single molecule fluorescence processivity assays showed that NKin is a processive motor. In agreement with previous work on the processivity of animal kinesins (Crevel et al., 1999; Hackney, 1995) and the role of the dimeric nature of kinesin for processive motion (Crevel et al., 1999; Hackney, 1995; Hancock and Howard, 1998 and 1999; Jiang and Hackney, 1997), a view emerges in which the processivity of kinesin is linked to a ''head-over-head'' interaction within the dimer. This widely accepted view (Schief and Howard, 2001) has recently been challenged (Hua et al., 2002), and experiments with a natural, single-headed kinesin suggest that other mechanisms might contribute significantly to the processivity of kinesins (Kikkawa et al., 2000, 2001; Okada and Hirokawa, 1999, 2000). Our quantitative analysis of the processivity of HKin and NKin shows convincingly that NKin is at least twice as processive as HKin. An important question raised by this finding relates to understanding possible mechanisms and domains involved in controlling the processivity of kinesins.

Physiological basis of fast, processive movement

The high gliding speed of NKin in multiple molecule in vitro gliding assays raised the possibility that this motor might take double-sized steps. A step size of 16 nm would explain nicely the doubled processivity and increased gliding speed while maintaining most features of conventional animal kinesin. Interestingly, both HKin and NKin exhibit similar run times on the microtubule of ~1 s under saturating ATP conditions. But, as reported by Crevel et al. (1999), NKin has a step size of 8 nm. Thus, the observed increase in the rate of ATP turnover, k_{cat}, must be responsible for the faster gliding speed; k_{cat} for HKin is ~40–50 ATP/head/s and for Nkin ~75–85 ATP/head/s (Coy et al., 1999; Hackney, 1988; Kallipolitou et al., 2001; Vale et al., 1985).

Do we have any insights into why NKin is so fast and yet processive? From the studies of truncated *Drosophila melanogaster* conventional kinesin and NKin molecules (Gilbert et al., 1995, 1998; Hackney, 1994; Hackney, 1995; Kallipolitou et al., 2001), we know that the isolated motor domain turns over ATP very fast (96 ATP/head/s and 250 ATP/head/s, respectively). Addition of the neck domain to the isolated motor domain reduces the ATPase of NKin monomers substantially (24–27 ATP/head/s) and only dimerization of the motor by formation of a stable coiled coil (starting at amino acid residue 373 for conventional kinesin and at residue 391 for NKin) yields a fully processive motor with high ATPase turnover. Biochemical studies of truncation and deletion mutants (Gilbert et al., 1995; Grummt et al., 1998b; Hackney, 1995; Jiang and Hackney, 1997; Jiang et al., 1997; Kallipolitou et al., 2001) support the following hypothesis: the core motor's catalytic turnover, measured by the ATPase activity of the isolated (truncated) monomeric kinesin, provides an upper limit of the performance of the motor. In the dimeric motor, processive movement is achieved by the tight coupling of the two heads; thus, by clocking each other's ATPase cycle, the heads will be slowed down. The reduced ATP turnover of truncated, monomeric motor constructs with neck region suggests an inhibitory role of the neck domain (Kallipolitou et al., 2001). This inhibition is overcome by binding of the dimeric motor molecule to the microtubule, resulting in the coordinated catalytic activity of the two heads and processive movement. Further evidence for an inhibitory effect of the neck domain comes from 1), the high turnover rate (150 ATP/head/s) of a dimeric neck-deletion mutant of another fast fungal kinesin (*Syncephalastrum*) with large sequence homology to NKin (Grummt et al., 1998a,b), and 2), recent work on a point mutant in the neck region of NKin. Schäfer et al., (2003) showed that the NKinY362K point mutation in the neck abolishes tight coupling between the two heads, leading to slow motility and an ATP-hydrolysis at the maximal rate of 260 ATP/head/s. An inhibitory interaction of the motor with its neck domain might serve as an important physiological adaptation, as a cargo-bound (versus an unbound motor) kinesin is no longer inhibited by the backfolding of the tail region (Coy et al., 1999; Hackney et al., 1992; Hackney and Stock, 2000; Kirchner et al., 1999; Seiler et al., 1999, 2000). A cargo-bound motor that is not attached to (and moving along) a microtubule would, if no neck inhibition were to be present, rapidly hydrolyze ATP without doing any mechanical work.

The higher gliding speed of NKin, as compared to HKin, is therefore dependent on 1), the intrinsic properties of the motor domain (i.e., its catalytic activity) and 2), the rate of coupling between individual head domains. Based on the above discussion, we expect the neck domain to be of crucial importance. Crystallographic data by Song et al. (2001) point at a possible structural correlate for the high intrinsic ATPase activity of NKin's head. They speculate that the comparatively open ATP-binding pocket enables NKin to bind and exchange nucleotides more readily (Gilbert, 2001).

What mechanisms might influence NKin's processivity? Several experimental pieces of evidence hint at a direct interaction between the neck of the motor molecule and the flexible C-terminal portion—the so-called E-hook—of both

α- and β-tubulin in the microtubule. First evidence for this interaction came from cross-linking studies (Tucker and Goldstein, 1997). Subsequently, Wang and Sheetz (2000) characterized processive movement of kinesin- (and dynein-) coated beads on subtilisin-digested microtubules and showed that removal of the flexible C-terminus of tubulin (E-hook, negatively charged), reduces the run length, but not the gliding speed, of conventional kinesin. Therefore, they hypothesized that an electrostatic interaction of the positively charged neck domain of the motor molecule with the flexible E-hook of tubulin might either keep the motor attached to or properly positioned on the microtubule such that complete dissociation of the motor from the microtubule is less likely. The influence of the length (Romberg et al., 1998; Thorn et al., 2000) and/or the charge of the neck domain of conventional kinesin (Thorn et al., 2000) on processive movement supports this hypothesis. Furthermore, studies of a genetically modified (C351) naturally monomeric kinesin, KIF1A, showed that a tight electrostatic interaction of a lysine-rich region, the so-called K-loop, of the motor domain allowed the monomeric motor to move along microtubules in a quasiprocessive fashion (Kikkawa et al., 2000, 2001; Okada and Hirokawa, 1999, 2000), better described as a unilaterally biased diffusion. It is still unknown how strong this interaction with the microtubule is, and how much force can be produced by a monomeric KIF1A motor during processive motion. Okada and Hirokawa proposed a biased Brownian motion-based mechanism for this quasiprocessive motion of the motor. Although such a mechanism predicts that single KIF1A-motors will not be able to produce movement against a substantial force (unlike conventional kinesins), the KIF1A data do suggest potential electrostatic contributions on the interaction of kinesin and microtubules (Okada and Hirokawa, 2000). The increased processivity of NKin could therefore be due to an increased electrostatic interaction of the neck portion of NKin with the E-hook of the microtubule. In contrast to this hypothesis, the neck domain does not show an increase of positive charges compared to other conventional kinesins, but a decrease (overall charge of the neck is +4, +4, and 0 for HKin, *Drosophila* kinesin, and NKin, respectively).We suspect a more subtle mechanism to be at work in this case. Clearly, NKin has been shown to have unique properties in the neck domain (Kallipolitou et al., 2001). One might actually argue that the reduced positive charge facilitates the dissociation of motor-microtubule interaction, thus allowing the rate of turnover during processive movement to increase without rendering the motor less processive. Because fungal kinesins have a conserved but different residue organization in the neck domain, we suggest that the processivity of NKin might be substantially influenced by its neck domain. Further studies of the processivity of the fungal kinesins with subtilisin-digested microtubules should now be conducted to gain further insights into the potential role of electrostatic interactions in the motile mechanism of kinesins.

We acknowledge technical support from Franz Schwarz and Sabine Fuchs. This work was support by grants from the Deutsche Forschungsgemeinschaft (ME1414/4-2 and SFB 413) and the Volkswagen Stiftung (I/74349).

REFERENCES

Becker, R. A., J. M. Chambers, and A. R. Wilks. 1988. The New S Language. Wadsworth and Brooks/Cole, Pacific Grove, CA.

Block, S. M., L. S. Goldstein, and B. J. Schnapp. 1990. Bead movement by single kinesin molecules studied with optical tweezers. *Nature*. 348: 348–352.

Bloom, G. S., M. C. Wagner, K. K. Pfister, and S. T. Brady. 1988. Native structure and physical properties of bovine brain kinesin and identification of the ATP-binding subunit polypeptide. *Biochemistry*. 27:3409–3416.

Brady, S. T. 1985. A novel brain ATPase with properties expected for the fast axonal transport motor. *Nature*. 317:73–75.

Coy, D. L., W. O. Hancock, M. Wagenbach, and J. Howard. 1999. Kinesin's tail domain is an inhibitory regulator of the motor domain. *Nat. Cell Biol.* 1:288–292.

Coy, D. L., M. Wagenbach, and J. Howard. 1999. Kinesin takes one 8-nm step for each ATP that it hydrolyzes. *J. Biol. Chem.* 274:3667–3671.

Crevel, I., N. Carter, M. Schliwa, and R. Cross. 1999. Coupled chemical and mechanical reaction steps in a processive Neurospora kinesin. *EMBO J.* 18:5863–5872.

Crevel, I. M., A. Lockhart, and R. A. Cross. 1997. Kinetic evidence for low chemical processivity in ncd and Eg5. *J. Mol. Biol.* 273:160–170.

de Cuevas, M., T. Tao, and L. S. Goldstein. 1992. Evidence that the stalk of Drosophila kinesin heavy chain is an alpha-helical coiled coil. *J. Cell Biol.* 116:957–965.

Foster, K. A., and S. P. Gilbert. 2000. Kinetic studies of dimeric Ncd: evidence that Ncd is not processive. *Biochemistry*. 39:1784–1791.

Funatsu, T., Y. Harada, H. Higuchi, M. Tokunaga, K. Saito, Y. Ishii, R. D. Vale, and T. Yanagida. 1997. Imaging and nano-manipulation of single biomolecules. *Biophys. Chem.* 68:63–72.

Gilbert, S. P. 2001. High-performance fungal motors. *Nature*. 414:597–598.

Gilbert, S. P., M. L. Moyer, and K. A. Johnson. 1998. Alternating site mechanism of the kinesin ATPase. *Biochemistry*. 37:792–799.

Gilbert, S. P., M. R. Webb, M. Brune, and K. A. Johnson. 1995. Pathway of processive ATP hydrolysis by kinesin. *Nature*. 373:671–676.

Grummt, M., S. Pistor, F. Lottspeich, and M. Schliwa. 1998a. Cloning and functional expression of a 'fast' fungal kinesin. *FEBS Lett*. 427:79–84.

Grummt, M., G. Woehlke, U. Henningsen, S. Fuchs, M. Schleicher, and M. Schliwa. 1998b. Importance of a flexible hinge near the motor domain in kinesin-driven motility. *EMBO J.* 17:5536–5542.

Hackney, D. D. 1994. Evidence for alternating head catalysis by kinesin during microtubule-stimulated ATP hydrolysis. *Proc. Natl. Acad. Sci. USA*. 91:6865–6869.

Hackney, D. D. 1995. Highly processive microtubule-stimulated ATP hydrolysis by dimeric kinesin head domains. *Nature*. 377:448–450.

Hackney, D. D. 1988. Kinesin ATPase: rate-limiting ADP release. *Proc. Natl. Acad. Sci. USA*. 85:6314–6318.

Hackney, D. D., J. D. Levitt, and J. Suhan. 1992. Kinesin undergoes a 9 S to 6 S conformational transition. *J. Biol. Chem.* 267:8696–8701.

Hackney, D. D., and M. F. Stock. 2000. Kinesin's IAK tail domain inhibits initial microtubule-stimulated ADP release. *Nat. Cell Biol.* 2:257–260.

Hancock, W. O., and J. Howard. 1998. Processivity of the motor protein kinesin requires two heads. *J. Cell Biol.* 140:1395–1405.

Hancock, W. O., and J. Howard. 1999. Kinesin's processivity results from mechanical and chemical coordination between the ATP hydrolysis cycles of the two motor domains. *Proc. Natl. Acad. Sci. USA*. 96:13147–13152.

Henningsen, U., and M. Schliwa. 1997. Reversal in the direction of movement of a molecular motor. *Nature*. 389:93–96.

Hirokawa, N., K. K. Pfister, H. Yorifuji, M. C. Wagner, S. T. Brady, and G. S. Bloom. 1989. Submolecular domains of bovine brain kinesin identified by electron microscopy and monoclonal antibody decoration. *Cell*. 56:867–878.

Howard, J., A. J. Hudspeth, and R. D. Vale. 1989. Movement of microtubules by single kinesin molecules. *Nature*. 342:154–158.

Howard, J., A. J. Hunt, and S. Baek. 1993. Assay of microtubule movement driven by single kinesin molecules. *Methods Cell Biol*. 39: 137–147.

Hua, W., J. Chung, and J. Gelles. 2002. Distinguishing inchworm and hand-over-hand processive kinesin movement by neck rotation measurements. *Science*. 295:844–848.

Hunt, A. J., F. Gittes, and J. Howard. 1994. The force exerted by a single kinesin molecule against a viscous load. *Biophys. J*. 67:766–781.

Hunt, A. J., and J. Howard. 1993. Kinesin swivels to permit microtubule movement in any direction. *Proc. Natl. Acad. Sci. USA*. 90:11653–11657.

Inoue, Y., Y. Y. Toyoshima, A. H. Iwane, S. Morimoto, H. Higuchi, and T. Yanagida. 1997. Movements of truncated kinesin fragments with a short or an artificial flexible neck. *Proc. Natl. Acad. Sci. USA*. 94: 7275–7280.

Jiang, M. Y., and M. P. Sheetz. 1995. Cargo-activated ATPase activity of kinesin. *Biophys. J*. 68 (Suppl):283S–285S.

Jiang, W., and D. D. Hackney. 1997. Monomeric kinesin head domains hydrolyze multiple ATP molecules before release from a microtubule. *J. Biol. Chem*. 272:5616–5621.

Jiang, W., M. F. Stock, X. Li, and D. D. Hackney. 1997. Influence of the kinesin neck domain on dimerization and ATPase kinetics. *J. Biol. Chem*. 272:7626–7632.

Kallipolitou, A., D. Deluca, U. Majdic, S. Lakamper, R. Cross, E. Meyhofer, L. Moroder, M. Schliwa, and G. Woehlke. 2001. Unusual properties of the fungal conventional kinesin neck domain from Neurospora crassa. *EMBO J*. 20:6226–6235.

Kikkawa, M., Y. Okada, and N. Hirokawa. 2000. 15 A resolution model of the monomeric kinesin motor, KIF1A. *Cell*. 100:241–252.

Kikkawa, M., E. P. Sablin, Y. Okada, H. Yajima, R. J. Fletterick, and N. Hirokawa. 2001. Switch-based mechanism of kinesin motors. *Nature*. 411:439–445.

Kirchner, J., S. Seiler, S. Fuchs, and M. Schliwa. 1999. Functional anatomy of the kinesin molecule in vivo. *EMBO J*. 18:4404–4413.

Kojima, H., E. Muto, H. Higuchi, and T. Yanagida. 1997. Mechanics of single kinesin molecules measured by optical trapping nanometry. *Biophys. J*. 73:2012–2022.

Kozielski, F., S. Sack, A. Marx, M. Thormahlen, E. Schonbrunn, V. Biou, A. Thompson, E. M. Mandelkow, and E. Mandelkow. 1997. The crystal structure of dimeric kinesin and implications for microtubule-dependent motility. *Cell*. 91:985–994.

Larson, H. J. 1982. Introduction to Probability Theory and Statistical Inference. John Wiley & Sons, New York.

Mehta, A. 2001. Myosin learns to walk. *J. Cell Sci*. 114:1981–1998.

Mehta, A. D., R. S. Rock, M. Rief, J. A. Spudich, M. S. Mooseker, and R. E. Cheney. 1999. Myosin-V is a processive actin-based motor. *Nature*. 400:590–593.

Meyhöfer, E., and J. Howard. 1995. The force generated by a single kinesin molecule against an elastic load. *Proc. Natl. Acad. Sci. USA*. 92:574–578.

Okada, Y., and N. Hirokawa. 1999. A processive single-headed motor: kinesin superfamily protein KIF1A. *Science*. 283:1152–1157.

Okada, Y., and N. Hirokawa. 2000. Mechanism of the single-headed processivity: diffusional anchoring between the K-loop of kinesin and the C terminus of tubulin. *Proc. Natl. Acad. Sci. USA*. 97:640–645.

Pierce, D. W., N. Hom-Booher, and R. D. Vale. 1997. Imaging individual green fluorescent proteins. *Nature*. 388:338.

Pierce, D. W., and R. D. Vale. 1998. Assaying processive movement of kinesin by fluorescence microscopy. *Methods Enzymol*. 298:154–171.

Rice, S., A. W. Lin, D. Safer, C. L. Hart, N. Naber, B. O. Carragher, S. M. Cain, E. Pechatnikova, E. M. Wilson-Kubalek, M. Whittaker, E. Pate, R. Cooke, E. W. Taylor, R. A. Milligan, and R. D. Vale. 1999. A structural change in the kinesin motor protein that drives motility. *Nature*. 402:778–784.

Romberg, L., D. W. Pierce, and R. D. Vale. 1998. Role of the kinesin neck region in processive microtubule-based motility. *J. Cell Biol*. 140:1407–1416.

Romberg, L., and R. D. Vale. 1993. Chemomechanical cycle of kinesin differs from that of myosin. *Nature*. 361:168–170.

Schäfer, F., Deluca, D., Majdic, U., Kirchner, J., Schliwa, M., Moroder, L., and G. Woehlke. 2003. A conserved tryrosine in the neck of fungal kinesin regulates the catalytic motor care. *Embo. J*. 22: In press.

Schief, W. R., and J. Howard. 2001. Conformational changes during kinesin motility. *Curr. Opin. Cell Biol*. 13:19–28.

Scholey, J. M., J. Heuser, J. T. Yang, and L. S. Goldstein. 1989. Identification of globular mechanochemical heads of kinesin. *Nature*. 338:355–357.

Seiler, S., J. Kirchner, C. Horn, A. Kallipolitou, G. Woehlke, and M. Schliwa. 2000. Cargo binding and regulatory sites in the tail of fungal conventional kinesin. *Nat. Cell Biol*. 2:333–338.

Seiler, S., M. Plamann, and M. Schliwa. 1999. Kinesin and dynein mutants provide novel insights into the roles of vesicle traffic during cell morphogenesis in Neurospora. *Curr. Biol*. 9:779–785.

Song, Y. H., A. Marx, J. Muller, G. Woehlke, M. Schliwa, A. Krebs, A. Hoenger, and E. Mandelkow. 2001. Structure of a fast kinesin: implications for ATPase mechanism and interactions with microtubules. *EMBO J*. 20:6213–6225.

Steinberg, G., and M. Schliwa. 1995. The Neurospora organelle motor: a distant relative of conventional kinesin with unconventional properties. *Mol. Biol. Cell*. 6:1605–1618.

Steinberg, G., and M. Schliwa. 1996. Characterization of the biophysical and motility properties of kinesin from the fungus Neurospora crassa. *J. Biol. Chem*. 271:7516–7521.

Svoboda, K., C. F. Schmidt, B. J. Schnapp, and S. M. Block. 1993. Direct observation of kinesin stepping by optical trapping interferometry. *Nature*. 365:721–727.

Thorn, K. S., J. A. Ubersax, and R. D. Vale. 2000. Engineering the processive run length of the kinesin motor. *J. Cell Biol*. 151:1093–1100.

Tomishige, M., and R. D. Vale. 2000. Controlling kinesin by reversible disulfide cross-linking. Identifying the motility-producing conformational change. *J. Cell Biol*. 151:1081–1092.

Tripet, B., R. D. Vale, and R. S. Hodges. 1997. Demonstration of coiled-coil interactions within the kinesin neck region using synthetic peptides. Implications for motor activity. *J. Biol. Chem*. 272:8946–8956.

Tucker, C., and L. S. Goldstein. 1997. Probing the kinesin-microtubule interaction. *J. Biol. Chem*. 272:9481–9488.

Vale, R. D., T. Funatsu, D. W. Pierce, L. Romberg, Y. Harada, and T. Yanagida. 1996. Direct observation of single kinesin molecules moving along microtubules. *Nature*. 380:451–453.

Vale, R. D., T. S. Reese, and M. P. Sheetz. 1985. Identification of a novel force-generating protein, kinesin, involved in microtubule-based motility. *Cell*. 42:39–50.

Venables, W. N., and B. D. Ripley. 1997. Modern Applied Statistics with S-Plus. Springer-Verlag, New York.

Verhey, K. J., and T. A. Rapoport. 2001. Kinesin carries the signal. *Trends Biochem. Sci*. 26:545–550.

Visscher, K., M. J. Schnitzer, and S. M. Block. 1999. Single kinesin molecules studied with a molecular force clamp. *Nature*. 400:184–189.

Wang, Z., and M. P. Sheetz. 2000. The C-terminus of tubulin increases cytoplasmic dynein and kinesin processivity. *Biophys. J*. 78:1955–1964.

Yang, J. T., R. A. Laymon, and L. S. Goldstein. 1989. A three-domain structure of kinesin heavy chain revealed by DNA sequence and microtubule binding analyses. *Cell*. 56:879–889.